Bioinspired Oxidation Catalysis

DOI: 10.1002/anie.200901865

Stereospecific C–H Oxidation with H_2O_2 Catalyzed by a Chemically Robust Site-Isolated Iron Catalyst**

Laura Gómez, Isaac Garcia-Bosch, Anna Company, Jordi Benet-Buchholz, Alfonso Polo, Xavier Sala, Xavi Ribas, and Miquel Costas**

Alkane functionalization stands as the bottleneck for the chemical elaboration of hydrocarbon feedstocks, and methodologies for stereospecific C–H bond oxidation can also open novel and more direct synthetic strategies towards complex organic molecules.[1] However, the inert nature of non-activated C–H bonds poses incomparable difficulties related to selectivity, and most common methodologies require the use of large excesses of substrate relative to oxidant to minimize overoxidation reactions. Not surprisingly, only a few systems affording synthetically useful yields have been described.[2,3,4c] Selected bioinspired nonheme iron complexes such as $[Fe(CH_3CN)_2(mep)]^{2+}$ (**1**; mep = *N*,*N*′-dimethyl-*N*,*N*′-bis(2-pyridylmethyl)ethylene-1,2-diamine; Scheme 1) are particularly attractive oxidation catalysts because they use H_2O_2 as oxidant and operate under mild conditions, although they commonly afford very modest product yields.[3] Chen and White recently reported a novel catalyst $[Fe(CH_3CN)_2((S,S)\text{-bpbp})]^{2+}$ (**2**; (*S*,*S*)-bpbp = 2-[{(*S*)-2-[((*S*)-1-pyridin-2-ylmethyl)pyrrolidin-2-yl]pyrrolidin-1-yl}-methyl]pyridine) that in the presence of acetic acid catalyzes the hydroxylation of complex organic molecules in a predictable manner and with synthetically useful yields.[4c] Their landmark system uses 15% catalyst loadings, and even though it affords very modest turnover numbers (2–6), efficiencies were substantially better than in any previously reported nonheme catalyst. The strong dependence between catalytic efficiency and small changes in the architecture of related catalysts is currently a challenge,[4] and strategies for improvement remain to be developed. To this end, we report herein the rational design of a very active iron catalyst for the stereospecific and site-predictable hydroxylation of alkanes with H_2O_2 to afford oxidized products in synthetically useful yields.

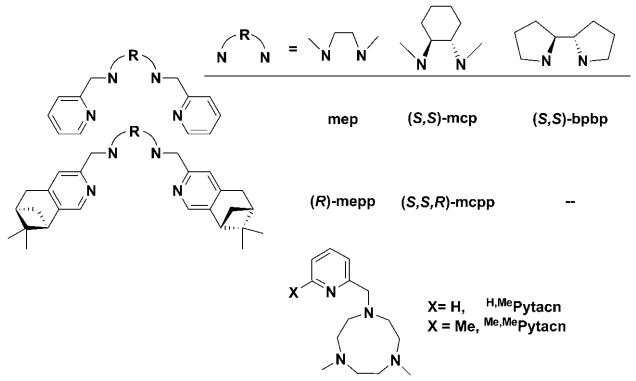

Scheme 1. Schematic representation of the ligands used in this study.

Our strategy was based on well-established principles in oxidation catalysis with heme complexes.[5] The introduction of aryl groups at the porphyrin meso positions isolates the metal site, which in turn limits bimolecular self-decomposition pathways and enhances the catalytic activity of the complexes by precluding formation of noncatalytic oxo dimers. We reasoned that analogous principles may apply to nonheme iron complexes. Although apparently simple, this strategy is made challenging by the known counterproductive modifications on the 6-position of the pyridine rings of polypyridyl iron complexes.[4g] Consequently, we targeted modification at a more remote position of the pyridine ring with a bulky hydrocarbon as a general strategy towards the design of a catalyst in which the iron site will be embedded in an oxidatively robust cavity. On the basis of this premise, (*S*,*S*,*R*)-mcpp, (*R*,*R*,*R*)-mcpp, and (*R*)-mepp ligands (Scheme 1) were targeted because they are structurally related to **1** and **2** and contain bulky pinene groups that help to isolate the iron site without perturbing its stability. In addition, for (*S*,*S*,*R*)-mcpp and (*R*,*R*,*R*)-mcpp, the chiral *trans*-1,2-cyclohexane diamine backbone imparts rigidity at the ligand, which allows predetermination of the topological chirality[6] and determines the relative orientation of the robust pinene CH_3 groups with respect to the metal site. To this end, C_2-symmetric complexes $[Fe(CF_3SO_3)_2(L)]$, [L = (*S*,*S*,*R*)-mcpp (**3**); (*R*,*R*,*R*)-mcpp (**4**); (*R*)-mepp (**5**)] were prepared by treatment of the corresponding tetradentate ligand with iron(II) chloride and subsequent reaction with 2 equivalents of AgOTf (see the Supporting Information).[7]

Figure 1 shows an ellipsoid diagram of the solid-state molecular structure of **3**,[8] which reveals that the coordination geometry of the Fe center is distorted octahedral with the

[*] L. Gómez, I. Garcia-Bosch, Dr. A. Company,[+] Dr. A. Polo, Dr. X. Ribas, Dr. M. Costas
Departament de Química, Universitat de Girona
Campus de Montilivi, 17071 Girona (Spain)
E-mail: xavi.ribas@udg.edu
miquel.costas@udg.edu
Dr. J. Benet-Buchholz, Dr. X. Sala
Institute of Chemical Research of Catalonia (ICIQ)
Av. Països Catalans 16, 43007 Tarragona (Spain)
[+] Current address: Technische Universität Berlin, Institut für Chemie (Germany)

[**] Financial support was provided by MCYT of Spain through projects CTQ2006-05367/BQU to M.C. L.G., A.C., and I.G.B. thank MICINN for PhD grants.

Supporting information for this article is available on the WWW under http://dx.doi.org/10.1002/anie.200901865.

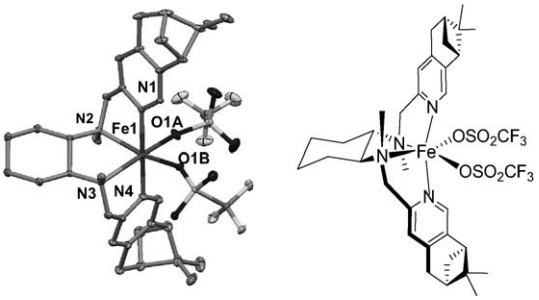

Figure 1. ORTEP (50% probability) diagram[8] (left), and chemical diagram (right) of [Fe(CF_3SO_3)$_2$((*S,S,R*)-mcpp)] (**3**). Hydrogen atoms are omitted for clarity.

ligand adopting a *cis*-α topology.[6] The nitrogen atoms of the two pyridine rings are disposed *trans* to each other, and the two aliphatic nitrogen atoms are situated *cis* relative to each other.

The complexes were tested as catalysts (1 mol%) for the hydroxylation of *cis*-1,2-dimethylcyclohexane (*cis*-DMCH) using H_2O_2 (1.2 equiv) as oxidant (Scheme 2, Table 1). Confirming our expectations, **3** (Table 1, entry 3) and **5** (Table 1, entry 5) proved to be the most efficient catalysts, and the former affords the corresponding tertiary alcohol in 57% yield (79% substrate conversion) with excellent stereoretention (99% *cis*). This yield is significantly better than those obtained with structurally related complexes **1** and **6**, which lack the pinene arms (Table 1, entries 1 and 6). The tacn-based iron complex **7** afforded a very low yield (Table 1, entry 7), but **8** and dipyrrolidine-based **2**, which have been reported as exceptionally active catalysts,[4b,c] provided the corresponding alcohol in 45% yield (Table 1, entries 8 and 2). Finally, since selective C–H hydroxylation reactions have been reported for manganese-based complexes,[9c–d] **9**[9e] and **10**[9a,b] were also tested, but proved not to be efficient (Table 1, entries 9 and 10).

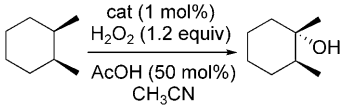

Scheme 2. Stereospecific hydroxylation of *cis*-DMCH.

Table 1: Oxidation of *cis*-DMCH by various catalysts.[a]

Entry	Catalyst	Yield [%][b]
1	[Fe(CF_3SO_3)$_2$(mep)] (**1**)	38
2	[Fe(CF_3SO_3)$_2$((*S,S*)-bpbp)] (**2**)	45
3	[Fe(CF_3SO_3)$_2$((*S,S,R*)-mcpp)] (**3**)	57
4	[Fe(CF_3SO_3)$_2$((*R,R,R*)-mcpp)] (**4**)	17
5	[Fe(CF_3SO_3)$_2$((*R*)-mepp)] (**5**)	49
6	[Fe(CF_3SO_3)$_2$((*S,S*)-mcp)] (**6**)	36
7	[Fe(CF_3SO_3)$_2$(^{H,Me}Pytacn)] (**7**)	2
8	[Fe(CF_3SO_3)$_2$(^{Me,Me}Pytacn)] (**8**)	45
9	[Mn(CF_3SO_3)$_2$((*S,S*)-mcp)] (**9**)	1
10	[Mn(CF_3SO_3)$_2$(^{H,Me}Pytacn)] (**10**)	8

[a] Cat/H_2O_2/substrate/AcOH 1:120:100:50. [b] Yields from GC based on product formed.

Table 2: Alkane oxidation reactions catalyzed by **3**.[a]

Entry	Substrate	Products	Yield [%]
1	*c*-C_6H_{12}	*c*-$C_6H_{10}O$	70[c]
2	*c*-C_6D_{12}	*c*-$C_6D_{10}O$	63[c]
3[b]	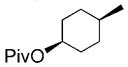	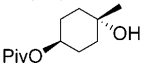	69[c] (57[d]) (51[e])
4	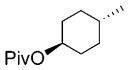	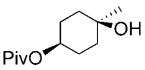 + 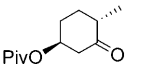	50[c] (39[d]) 19[c] (16[d])

[a] Cat/H_2O_2/substrate/AcOH 1:120:100:50 followed by a second addition of cat/H_2O_2/AcOH 1:120:50. [b] Third addition of cat/H_2O_2/AcOH 1:120:50. [c] Yield from GC. [d] Yield of isolated product. [e] Yield for **2** from GC under the same conditions (analogous yield was obtained when [Fe(CH_3CN)$_2$((*S,S*)-bpbp)](SbF_6)$_2$ (**2**-SbF_6) was used as catalyst).

Overall, these efficiencies compare well with reported copper and iron based systems that work via free-radical type intermediates,[12] although the stereospecificity and regioselectivity (see below) observed in the hydroxylation reactions mediated by **3** rather suggest the involvement of highly selective high-valent iron–oxo species.[4b,e,g,13]

The stereospecific hydroxylation of tertiary C–H bonds was also explored, since it opens an entry to trisubstituted chiral alcohols, which is not amenable for free diffusing radical-type reactions. A series of substrates (Table 2 and Schemes 3 and 4) were oxidized to the corresponding alcohols

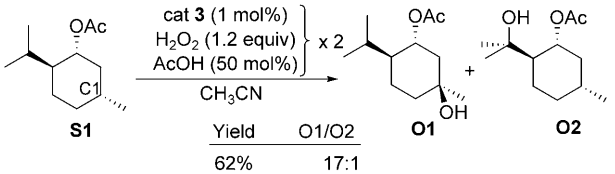

Scheme 3. Regiospecific oxidation of (−)-acetoxy-*p*-menthane **S1**.

in 35–69% yields. In general, the catalyst exhibits a good selectivity for tertiary C–H bonds, even in the presence of statistically more important secondary C–H sites. This preference for tertiary positions indicates that the strength of the C–H bond is a major factor in dictating site selectivity, and it is consistent with an oxidant that operates by hydrogen atom abstraction. More significantly, as observed for *cis*-DMCH, the oxidations are stereospecific (Table 2, entries 3

and 4), indicating that long-lived carbocationic or radical-type intermediates are not involved. Electronic and steric factors play a role in discriminating between different C–H bonds, thus making site-selective oxidation predictable. The role of steric factors was established by performing the oxidation of (−)-acetoxy-*p*-menthane (**S1**; Scheme 3). Hydroxylation preferentially occurs (17:1, 62% yield by GC and 50% yield of isolated product) in the more accessible (C1)–H bond to give product **O1**. In contrast, hydroxylation of **S1** by **6**, **2**-SbF_6, **1**, **5**, and **8** under analogous low catalyst loading conditions affords **O1** in only 6% (up to 37% if a ratio (cat/H_2O_2/AcOH 5:120:50) × 3 is used), 31%, 6%, 26%, and 34% yields, respectively.[14] Electronic effects are clearly evidenced when the oxidation of substrates containing multiple C–H bonds is attempted (Scheme 4). Oxidation of 2,6-dimethyloctane

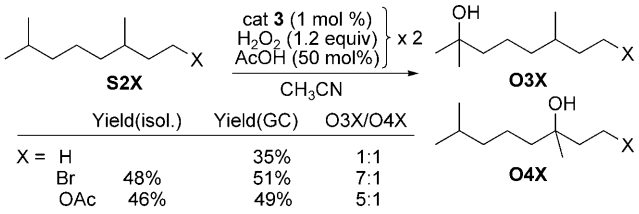

Scheme 4. Electronic discrimination in the oxidation of substrates with multiple tertiary C–H bonds.

(**S2H**) affords a 1:1 mixture of tertiary alcohol products (**O3H** and **O4H**), whereas functionalization of **S2Br** and **S2OAc** occurs selectively at the distal C–H bond.

The profound effect that the bulky pinene groups have in the efficiency and stability of the catalysts is evidenced by performing a time-profile analysis of the oxidation of **S1** catalyzed by **3** and **6** (Figure 2), which indicates that the H_2O_2 oxidant is more rapidly and efficiently consumed by **3**, and that unlike **6**, **3** is not substantially deactivated during the reaction. A second addition of H_2O_2 and **S1** resumes the catalytic activity of **3**, but not of **6**. Effectively, ESI-MS analyses (Figures S6 and S7 in the Supporting Information) show that monomeric $[LFe^{III}(OR)(CF_3SO_3)]^+$ (OR = OH, OAc) species, which are presumed to be the precursors of the high-valent iron–oxo species responsible for catalytic activity,[4b,e,g,13] still remain in final reaction solutions of **3**, whereas they rapidly disappear during H_2O_2 addition when **6** is used.

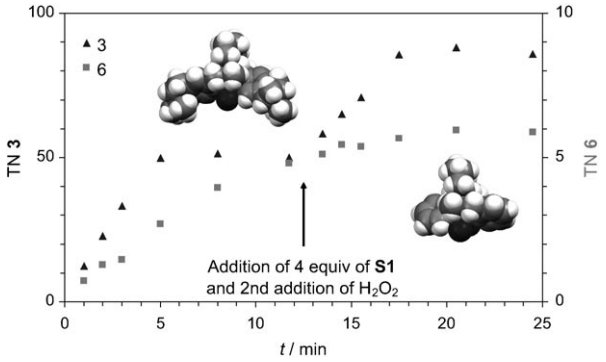

Figure 2. **O1** formation (turnover number; TN) versus time in the catalytic oxidation of **S1** by **6** and **3**. Note that the *y* scales for the data for each catalyst are different. Inset: Space-filling XRD diagrams of **3** (left), and the (*R*,*R*)-isomer of **6**[15] (right). CF_3SO_3 groups (except for the O atom, in black, directly bound to Fe) have been removed for clarity.

Analysis of the molecular structures of **3**[8] and **6**[15] (Figure 1 and insets in Figure 2) reveals key aspects that help to explain the remarkable catalytic activity exhibited by **3**. The iron site in **3** is embedded in a well-defined chiral hydrophobic pocket, but is fully exposed in **6**. In addition, the predetermined chirality imposed by the *trans*-(1*S*,2*S*)-diaminocyclohexane backbone positions the very robust (−)-pinene CH_3 groups of **3** pointing towards the metal site. We conclude that this steric bulk most likely helps to prevent formation of noncatalytic oxo dimers and oligomeric species,[16] and can also limit bimolecular decomposition pathways, thus explaining its enhanced catalytic activity.

In conclusion, **3** constitutes the most active and efficient nonheme iron hydroxylation catalyst reported so far. It compares with state-of-the-art C–H hydroxylation systems in terms of product yields, selectivity, and predictability; it requires low catalyst loadings and makes efficient use of H_2O_2. We envision that further use of the principle of steric isolation, combined with an oxidatively robust site, may led to the design of even more active catalysts that could open the door to environmentally benign synthetic strategies based on C–H hydroxylation.

Experimental Section

Full experimental details for the preparation of the complexes, and for catalytic oxidation reactions are included in the Supporting Information.

Received: April 7, 2009
Published online: June 27, 2009

Keywords: catalyst design · homogeneous catalysis · hydrogen peroxide · iron · oxidation

[1] a) G. Dyker, *Handbook of C-H Transformations, Vol. 1–2*, Wiley-VCH, Weinheim, **2005**; b) J. A. Labinger, J. E. Bercaw, *Nature* **2002**, *417*, 507–514; c) H. M. L. Davies, J. R. Manning, *Nature* **2008**, *451*, 417–424; d) R. G. Bergman, *Nature* **2007**, *446*, 391–393; e) K. Godula, D. Sames, *Science* **2006**, *312*, 67–72.

[2] a) R. W. Murray, R. Jeyaraman, L. Mohan, *J. Am. Chem. Soc.* **1986**, *108*, 2470–2472; b) R. Mello, M. Fiorentino, C. Fusco, R. Curci, *J. Am. Chem. Soc.* **1989**, *111*, 6749–6757; c) G. Asensio, M. E. González-Núñez, C. B. Bernardini, R. Mello, W. Adam, *J. Am. Chem. Soc.* **1993**, *115*, 7250–7253; d) R. A. Periana, D. J. Taube, S. Gamble, H. Taube, T. Satoh, H. Fujii, *Science* **1998**, *280*, 560–564; e) S. Lee, P. L. Fuchs, *J. Am. Chem. Soc.* **2002**, *124*, 13978–13979; f) B. H. Brodsky, J. Du Bois, *J. Am. Chem. Soc.* **2005**, *127*, 15391–15393; g) A. R. Ekkati, J. J. Kodanko, *J. Am. Chem. Soc.* **2007**, *129*, 12390–12391; h) S.-M. Yiu, W.-L. Man, T.-C. Lau, *J. Am. Chem. Soc.* **2008**, *130*, 10821–10827.

[3] a) L. Que, Jr., W. B. Tolman, *Nature* **2008**, *455*, 333–340; b) A. Correa, O. G. Mancheño, C. Bolm, *Chem. Soc. Rev.* **2008**, *37*, 1108–1117; c) M. Costas, K. Chen, L. Que, Jr., *Coord. Chem. Rev.* **2000**, *200–202*, 517–544.

[4] Selected iron complexes as catalysts in C–H oxidation reactions: a) J. England, C. R. Davies, M. Banaru, A. J. P. White, G. J. P. Britovsek, *Adv. Synth. Catal.* **2008**, *350*, 883 – 897; b) A. Company, L. Gómez, X. Fontrodona, X. Ribas, M. Costas, *Chem. Eur. J.* **2008**, *14*, 5727 – 5731; c) M. S. Chen, C. M. White, *Science* **2007**, *318*, 783 – 787; d) J. England, G. J. P. Britovsek, N. Rabadia, A. J. P. White, *Inorg. Chem.* **2007**, *46*, 3752 – 3767; e) A. Company, L. Gómez, M. Güell, X. Ribas, J. M. Luis, L. Que, Jr., M. Costas, *J. Am. Chem. Soc.* **2007**, *129*, 15766 – 15767; f) V. B. Romakh, B. Therrien, G. Süss-Fink, G. B. Shul′pin, *Inorg. Chem.* **2007**, *46*, 3166 – 3175; g) K. Chen, L. Que, Jr., *J. Am. Chem. Soc.* **2001**, *123*, 6327 – 6337; h) G. Roelfes, M. Lubben, R. Hage, L. Que, Jr., B. L. Feringa, *Chem. Eur. J.* **2000**, *6*, 2152 – 2159.

[5] a) B. Meunier, *Chem. Rev.* **1992**, *92*, 1411 – 1456; b) J. L. McLain, J. Lee, J. T. Groves in *Biomimetic Oxidations Catalyzed by Transition Metal Complexes* (Ed.: B. Meunier), Imperial College Press, London, **2000**, pp. 91 – 169.

[6] U. Knof, A. von Zelewsky, *Angew. Chem.* **1999**, *111*, 312 – 333; *Angew. Chem. Int. Ed.* **1999**, *38*, 302 – 322.

[7] A. L. Sauers, D. M. Ho, S. Bernhard, *J. Org. Chem.* **2004**, *69*, 8910 – 8915; for previous reports on alkene and alkane oxidation catalysis with pineno–bipyridyl iron catalysts, see: a) C. Marchi-Delapierre, A. Jorge-Robin, A. Thibon, S. Ménage, *Chem. Commun.* **2007**, 1166 – 1168; b) Y. Mekmouche, C. Duboc-Toia, S. Ménage, C. Lambeaux, M. Fontecave, *J. Mol. Catal. A* **2000**, *156*, 85 – 89.

[8] CCDC 726566 (**3**) contains the supplementary crystallographic data for this paper. These data can be obtained free of charge from The Cambridge Crystallographic Data Centre via www.ccdc.cam.ac.uk/data_request/cif.

[9] a) I. Garcia-Bosch, A. Company, X. Fontrodona, X. Ribas, M. Costas, *Org. Lett.* **2008**, *10*, 2095 – 2098; b) I. Garcia-Bosch, X. Ribas, M. Costas, *Adv. Synth. Catal.* **2009**, *351*, 348 – 352; c) K. Nehru, S. J. Kim, I. Y. Kim, M. S. Seo, Y. Kim, S.-J. Kim, J. Kim, W. Nam, *Chem. Commun.* **2007**, 4623 – 4625; d) S. Das, C. D. Incarvito, R. H. Crabtree, G. W. Brudvig, *Science* **2006**, *312*, 1941 – 1943; e) A. Murphy, G. Dubois, T. D. P. Stack, *J. Am. Chem. Soc.* **2003**, *125*, 5250 – 5251.

[10] Under analogous conditions, **1**, **4**, and **6** afforded 15% (A/K = 0.22), 3% (A/K = 2), and 13% (A/K = 0.44) yields respectively.

[11] A third addition resulted in lower yields, presumably because of product overoxidation.

[12] a) G. Trettenhahn, M. Nagl, N. Neuwirth, V. B. Arion, W. Jary, P. Pöchlauer, W. Schmid, *Angew. Chem.* **2006**, *118*, 2860 – 2865; *Angew. Chem. Int. Ed.* **2006**, *45*, 2794 – 2798; b) A. M. Kirillov, M. N. Kopylovich, M. V. Kirillova, M. Haukka, M. F. C. Guedes da Silva, A. J. L. Pombeiro, *Angew. Chem.* **2005**, *117*, 4419 – 4423; *Angew. Chem. Int. Ed.* **2005**, *44*, 4345 – 4349; c) C. Pavan, J. Legros, C. Bolm, *Adv. Synth. Catal.* **2005**, *347*, 703 – 705; d) B. Retcher, J. Sánchez Costa, J. Tang, R. Hage, P. Gamez, J. Reedijk, *J. Mol. Catal. A* **2008**, *286*, 1 – 5.

[13] For a recent mechanistic study of the effect of the acetic acid in epoxidation reactions catalyzed by related iron complexes, see: R. Mas-Ballesté, L. Que, Jr., *J. Am. Chem. Soc.* **2007**, *129*, 15964 – 15972.

[14] A comparative time-profile analysis for the oxidation of **S1** by **2**-SbF_6, **3**, and **6** can be found as Figure S4 in the Supporting Information.

[15] M. Costas, A. K. Tipton, K. Chen, D.-H. Jo, L. Que, Jr., *J. Am. Chem. Soc.* **2001**, *123*, 6722 – 6723.

[16] Deactivation of **2** via formation of oligomeric species has been recently proposed; N. A. Vermeulen, M. S. Chen, M. C. White, *Tetrahedron* **2009**, *65*, 3078 – 3084.

